Carbon Trends 10 (2023) 100253

Contents lists available at ScienceDirect

Carbon Trends

journal homepage: www.elsevier.com/locate/cartre

A multidisciplinary approach to optimizing the mechanical characterization and dismantling of nuclear-grade graphite

Riccardo Chebac[a,*], Fabio Vanoni[a], Alessandro Porta[a], Fabrizio Campi[a], Alessandro Cocco[b], Silvia Barella[c], Andrea Gruttadauria[c]

[a] Politecnico di Milano, Department of Energy, Nuclear Engineering Division, Via La Masa 34, Milan 20156, Italy
[b] Politecnico di Milano, Department of Aerospace Science and Technology, Via La Masa 34, Milan 20156, Italy
[c] Politecnico di Milano, Department of Mechanical Engineering, Via La Masa 1, Milan 20156, Italy

A B S T R A C T

The large variability of the physical properties related to different types of nuclear-grade graphite makes its characterization for the decommissioning of nuclear power plants extremely problematic and time consuming. To facilitate this process, standardized procedures must be implemented taking into account the complexity of handling irradiated graphite. To this goal, the following study will present the mechanical tests chosen for a clear and easy characterization process. Virgin Atcheson Graphite Ordinary Temperature (AGOT), used as moderator and reflector in the L-54 M research reactor, has been used as a first attempt. Two standard mechanical tests are performed: uni-axial compression and four-point bending. Mechanical anisotropy of graphite was studied and verified, showing roughly a 30% difference between the machining directions parallel and perpendicular to the extrusion direction. A modified three-point bending test has been proposed, which may be used as a four-point bending substitute in case samples with non-standard geometries are needed. A correlation has been presented between the compressive, tensile strength and Young's modulus properties of graphite with Vickers microhardness with R2 respectively of 0.58, 0.53, and 0.91. Non-linear structural simulations of the tests have then been developed as supporting tools for retrieving additional mechanical information, such as Young's modulus. Finally, stress-strain curves have been used as input to develop a finite element method (FEM) which drastically improves the predictive capabilities by reducing the error from 102.2% to 27.6% for AGOT compressive strength, and from 16% to 0% AGOT tensile strength, when compared to in-built graphite models. The potential capabilities of this model to simulate potential graphite handling scenarios in the decommissioning process of nuclear power plants has been demonstrated.

1. Introduction

More than 200 commercial reactors and over 500 research reactors have been decommissioned worldwide. Technologies ranging from light-water reactors (LWR) up to fast breeder reactors (FBR) have all been successfully dismantled; all except graphite-moderated reactors [1]. Of this technology, only four decommissioning projects have currently been finalized with variable degrees of success: Fort St.Vrain [2], the Windscale advanced gas reactor [3], the Gleep reactor [4], and the Brookhaven National Laboratory Research Reactor [5]. Graphite has been extensively used as a moderator and reflector in various nuclear installations. According to data published in 2010 by the IAEA in TECDOC- 1647 [6], the world resources of i-graphite at that time were approximately 250,000 tons (160,000 m^3) with USA, UK, France, and Germany holding the most of it [7]. Graphite is also being considered as a key component of future reactors such as Molten-salt reactors (MSR), High-Temperature Gas Reactors (HTGR) and Fluoride-cooled High-Temperature Reactors (FHR) [8–12]. Nuclear grade graphite is a composite material manufactured from a filler coke and pitch binder [13,14]. The various types are usually manufactured from isotropic cokes such as petroleum or coal-tar. After carbonization, also referred to as baking, at temperatures greater than 2500 °C. The blocks are usually impregnated with a petroleum pitch and re-baked to densify the artifact. Impregnation and re-bake may occur several times to attain the required density. When dealing with irradiated graphite the three main hurdles are the volume of the waste, the presence of long-lived radionuclides [15], and the presence of Wigner energy [16]. This brings the projected cost of dismantling to be five times higher and produce ten times more volume of waste per MWh [17] compared to their LWR counterpart. To solve these issues, within the European H2020 Inno4Graph project [18], various tasks are being carried out to improve the knowledge of graphite behavior under irradiation and during dis- mantling operations to optimize the whole dismantling process. One of the main bottlenecks to overcome is the lengthy and expensive characterization phase prior to the decommissioning procedures [19]. This is particularly true when dealing with the characterization of the mechanical properties of graphite. As shown by Heijna et al. [20], graphite properties may vary significantly depending on manufacturing techniques and binder/filler choices. As such, graphite behavior under irradiation will be unique for each type and studies have to be made to assess the physical, chemical, and radiological properties of each one of them. In this work, a comprehensive study of the mechanical properties of AGOT graphite will be presented that is used as a moderator and reflector in the L-54 M research reactor located at the Politecnico di Milano. Many

* Corresponding author.
E-mail address: Riccardo.chebac@polimi.it (R. Chebac).

https://doi.org/10.1016/j.cartre.2023.100253
Received 28 November 2022; Received in revised form 17 February 2023; Accepted 17 February 2023

studies have been conducted on various types of nuclear-grade graphite, from Magnox Pile grade graphite to IG-110 and A3 [21] which will also be extensively used in Generation IV reactors [22]. AGOT graphite also has been studied by W.L. Greenstreet et al. [23] and Corum et al. [24]. In the following paper, a standardized methodology to be used as a benchmark for graphite types will be presented. L-54 M [25] is a research homogeneous-fuel thermal nuclear reactor fueled by a uranyl sulfate aqueous solution enriched to 19.94% in 235 U. Even though graphite has a theoretical density of 2.265 g/cm^3, the density for AGOT graphite is 1.6 g/cm^3 due to its inter-crystalline porosity given by the polycrystalline structure. This value is typical for first-generation graphite, while second- and third-generation have densities, of 1.7 g/cm^{3}and 1.8 g/cm^3 respectively [26]. The trend of increasing density is required to provide a higher core-specific power output [27] thanks to the improved moderation which increases the likelihood of neutron scattering and slowdown, reducing plant footprint and decreasing low and intermediate-level waste production. The following paper will look at the mechanical characterization of graphite and the procedures behind the tests chosen. For compressive strength, uni-axial compression test was deemed optimal. Given its self-lubricating properties and ceramic-like behavior [28,29], graphite is not suited for tensile tests. This is because high precision is needed while centering the specimen within the machine. Moreover, machining the graphite sample to the required geometry is extremely complicated, and usually, alternative solutions are adopted for the grabbing area. This leads to less precise results and higher costs (both for machining and decontamination of the machinery). Therefore, a four-point bending test was chosen as a more suitable setup [30]. The thought process that goes into decommissioning mainly revolves around minimizing waste and reducing the handling of radioactive material to as low as reasonably achievable [31]. To this extent, a further step was taken in the bending test to reduce the required machining of the samples even further and to minimize the cost of the experimental setup. Graphite-moderated reactors usually have zones within the core with graphite samples of predetermined dimensions that are inserted to be used for future tests after irradiation. The aim of this part of the study was to evaluate the possibility of using these samples of cylindrical geometry, as they are, within a bending test. This also allows having a similar specimen for both bending and compression tests, further reducing the complexity and waste production of the mechanical characterization. That is why a study of three-point bending was carried out to evaluate differences in the results with respect to the four-point bending test. A study on possible correlations between Vickers hardness and other mechanical properties will be provided, and a newly developed non-linear structural model will be discussed. Finally, a novel FEM model which represents an advancement over previous models that do not account for the asymmetry of the graphite stress-strain curve will be presented.

2. Experimental

The types of graphite studied were: AGOT graphite from the L-54 M reactor, nuclear-grade graphite from Latina, Vandellos-1 and Chinon A2 power reactors, and electrode-grade graphite. Microstructural analysis was performed via Scanning Electron Microscope (SEM) with a Zeiss Evo 50. The MTS Synergie 200 (maximum load 1 kN) was used for flexural and compression tests. The crosshead speed was set to 3 mm/min. Uniaxial compression tests were performed following ASTM C695–15 [32] on an MTS-150. AGOT and Latina graphite samples used for compression tests were machined into cylinders with 40 mm diameter and 80 mm height and parallel faces. The compression attachments used were the MTS 643.06B plates. For the four-point bending flexural test, AGOT and Latina graphite samples were machined into parallelepipeds with width (d) of 4 mm, depth (d) of 3 mm, and length of 40 mm. The setup was based on ASTM C651–20 [33]. The attachment was the Ceramic Bend fixture Model 642.05A-02 with a load span being 1/3 of the L support span measuring 30 mm. The stress was calculated via Eq. (1):

$$\sigma = \frac{FL}{bd^2} \tag{1}$$

For the modified three-point bending flexural test, AGOT samples were machined into cylinders with 6 mm diameters and 60 mm height. The fixture adopted was the MTS 642.01A . Four batches of specimens were produced: two cylindrical and two parallelepipeds. For each type, one batch was machined parallel to the direction of extrusion and one perpendicular. To evaluate the maximum stress in the sample, Eq. (1) cannot be used. Instead, Eq. (2) has to be considered:

$$\sigma = \frac{FL}{\pi r^3} \tag{2}$$

For Vickers microhardness, 10 mm wide and 4 mm thick disks were machined for AGOT, Latina, Chinon A2, Vandellos, and Electrode-grade graphite. The machine used was the Fischer 50–359. This device manages to separately calculate both Vickers microhardness and Young's modulus through indentation. Forces of indentation of both 500 mN and 1000 mN were studied with the former granting more accurate results, therefore, in the following only the former results will be discussed.

3. Mechanical tests

3.1. Compressive strength

To be compliant with the standards, any machined specimen is required to have its minimum dimension be at least five times greater than the average grain size [32]. This is necessary since results may vary with sample dimensions if they are comparable to grain size [34]. Therefore, a SEM analysis was carried out as verification. Fig. 1 shows images of

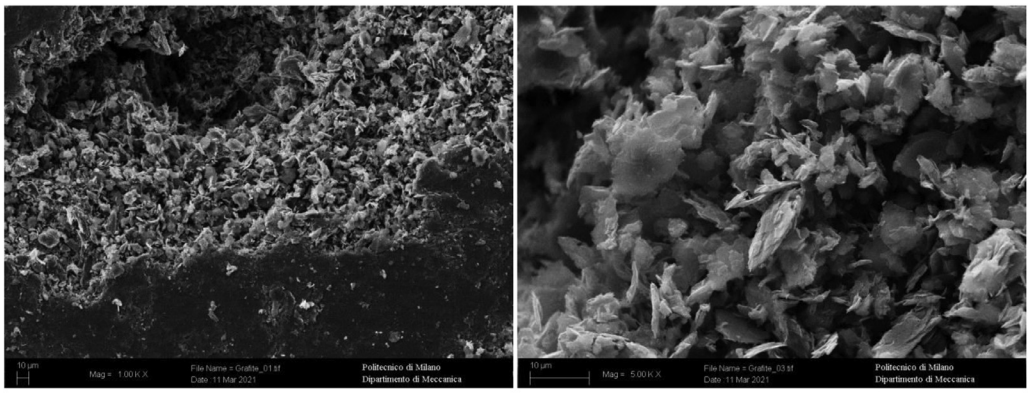

(a) (b)

Fig. 1. Images of graphite grains at different levels of magnification, growing from (a) to (b).

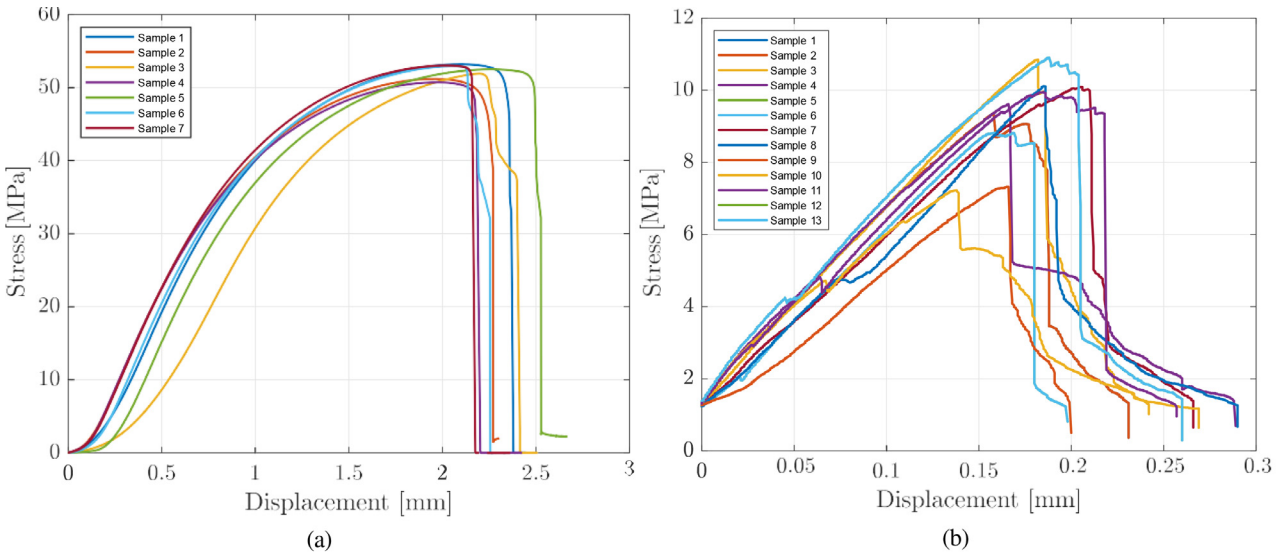

Fig. 2. Results of mechanical tests for (a) uni-axial compression and (b) four-point bending.

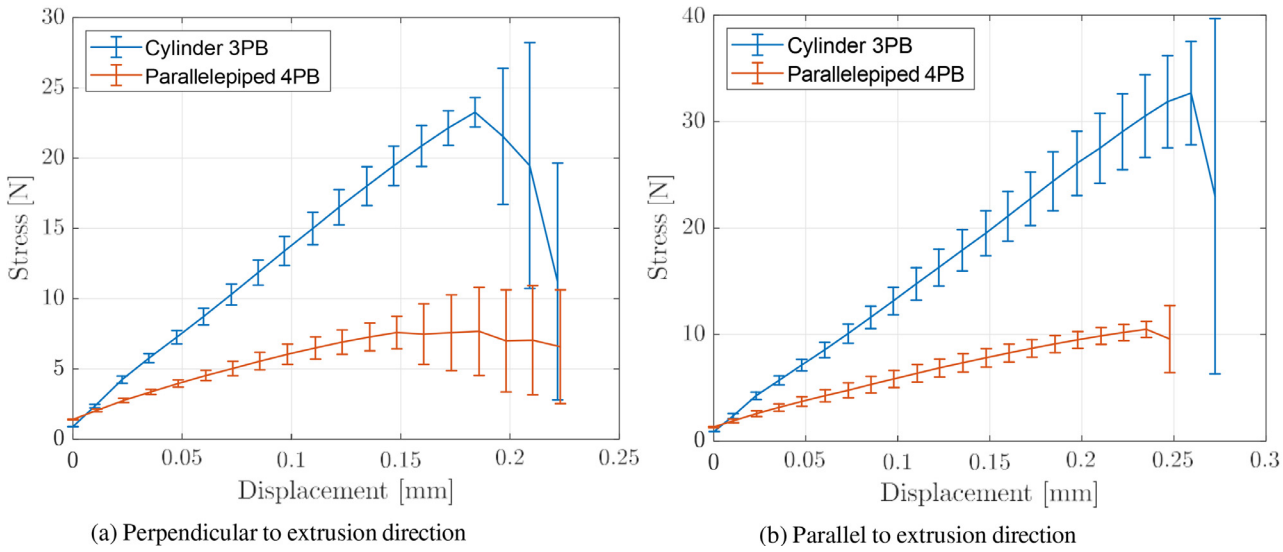

Fig. 3. Results of mechanical tests of cylinders in a three-point bending configuration and parallelepiped in four- point bending configuration.

AGOT graphite grains at different magnification levels. Grains hardly exceed 10 μm in size, putting it in between the superfine and ultra-fine graphite type as per the ASTM standard D8075–16 [35,36]. From SEM observations the morphology of the graphite results isotropic with grains having heterogeneous sizes and shapes which lead to porosities [37]. Fig. 2.a shows the results of uni-axial compressions undertaken for 7 cylindrical samples. Their extrusion direction of them was not known. The average maximum compressive stress of 52.025 ± 1.068 MPa. Both the stress- displacement curves as well as the 45° angle fracture highlights the ceramic-like behavior of graphite. The characteristic "S" shape of the stress-displacement curve shown is likely given by an inner re-arrangement of non-burnt binder and filler, with hydrocarbons still present within the graphite structure.

3.2. Bending tests

Fig. 2.b provides the results coming from the four-point bending tests. 13 parallelepiped samples were machined and information on the extrusion direction is not known. The maximum average tensile stress was found to be 8.72 ± 1.34 MPa, far lower than the compressive one, as expected by a quasi-ceramic material. The drawback of this test lies in the difficulty in retrieving the entire stress-strain curve. This could be possible by implementing a deflectometer which at the moment of the test was unavailable. Furthermore, the feasibility to modify a three-point bending flexural test to accommodate non-standard specimen size as well as the influence of extrusion direction on graphite properties is studied. The results given in Fig. 3 and summarized in Table 1, show a clear anisotropy in the mechanical behavior of AGOT graphite. The samples machined parallel to the extrusion direction have approximately 30% higher resistance to tension. Furthermore, three-point bending also shows higher resistance to tension, having 70% higher ultimate flexural

Table 1
Maximum stress reached in the various configurations.

Test	Geometry	Orientation	Maximum Stress [MPa]
3PB	Cylinder	Parallel	32.7
3PB	Cylinder	Horizontal	23.5
4PB	Parallelepiped	Parallel	10.6
4PB	Parallelepiped	Horizontal	7.7

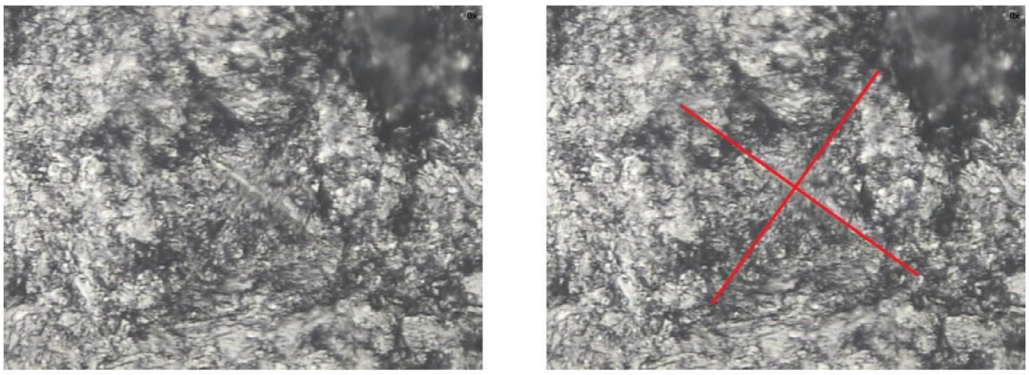

Fig. 4. Microscope image of the engraving done by the device for Vickers microhardness (left) and the highlighted diagonals of the engraver for hardness calculation (right).

Table 2
Correlations for Young's modulus, tensile and compressive strength to Vickers hardness (H_v).

Property	Correlation	R^2
Young's modulus [GPa]	0.158 Hv + 1.506	0.91
Tensile strength [MPa]	0.773 Hv + 7.528	0.53
Compressive Strength [MPa]	1.053 Hv + 19.770	0.58

Table 3
Vickers microhardness results at 500 mN force.

Graphite	H_v	Standard Error
L-54M	16.14	4.71
Vandellos	6.23	2.25
Chinon	12.24	2.12
Latina	4.14	1.75
Electrode	7.19	3.34

stress. Two main explanations were found for this overestimation: from a literature review [30,38], four-point bending has been proven to provide more accurate results for the bulk behavior compared to three-point bending since the area on which the maximum bending stress occurs happens to be between the two loading points whilst for three- point bending is localized and concentrated under the loading pin. This is particularly evident in non-homogeneous materials such as graphite. In addition, cylindrical geometries have lower stress concentration areas, further improving the maximum reachable stress. Therefore, the use of a three-point bending test is possible if combined with a suitable correction factor that takes into consideration what was previously discussed. For AGOT graphite the correction factor was found to be 3.05.

4. Mechanical properties correlation to Vickers hardness

This experimental campaign aimed to determine whether Vickers microhardness could be used as a gage to estimate the other mechanical properties. To do so, information on the compressive and tensile strength of Vandellos-1, Chinon A2, and electrode-grade graphite was also obtained. Young's modulus, tensile, and compressive strength have been corrected by the relative density to take into account variations of the properties given by porosity. As a reference, the theoretical density of graphite was considered to be 2.662 g/cm^3 [39,40]. The tests performed for Vickers micro hardness [41] are shown in Fig. 4 which were carried out by performing an indentation with a diamond indenter on the graphite surface. Via imaging software, the area of the sloping surface of the indentation was calculated by measuring the diagonals of the indentation and using the following equation:

$$HV = 1.854\frac{F}{d^2} \tag{3}$$

With F being the load applied in KgF and d the arithmetic average between the two diagonals. The results in Fig. 5 compare the mechanical properties of the graphite types to Vickers microhardness. The equation for each curve and the respective R2 are presented in Table 2, and in Table 3 the values of Vickers microhardness for all graphite types are given. The relative density correction provided a slight improvement of roughly 0.02 ÷ 0.04 to the R2 depending on the correlation. For the tensile correlation (Fig. 5.b), the linear curve was calculated excluding the point relative to L-54 M, which was considered an outlier. It can be seen that the properties which suffer the most from the directionality of the samples (i.e. compressive and tensile strength) are the ones with the lower R2 (respectively 0.58 and 0.53). Most likely, by taking into account this factor, more accurate correlations may be achievable.

5. Computational models

5.1. Structural model

A non-linear structural model based on a finite volume beam [42] was developed in MBDyn [43] to iteratively find Young's modulus that best fitted the experimental results. The model was developed to recreate both four-point bending and compressive tests. A good match was found with a Young modulus of 4.7 GPa, in line with the value derived from the Vickers microhardness test of 5.19 ± 0.74 and from literature [44]. To match the mean experimental curve obtained in the compression test, a simpler rod element was used with the constitutive law of Eq. (4):

$$\sigma = EA\left(0.853\epsilon - 1.95\cdot 10^8|\epsilon|\epsilon + 2.1\cdot 10^9\epsilon^3\right) \tag{4}$$

with E being Young's modulus, A the section area of the sample, and ϵ the strain. The coefficients of the cubic law are given by best fitting the curve with the experimental data. The results are shown in Fig. 6.

5.2. L-54 M graphite FEM model

The results from the mechanical tests were merged in the L-54 M graphite characteristic stress-strain curve (Fig. 7) which has been used as input for the FEM model in COMSOL Multiphysics software [45]. Since four-point bending test requires the use of a deflectometer, not available during the experimental campaign, to provide such a curve, a linear approximation using Young's modulus was calculated for the tension part of the plot. To evaluate the complete stress state, together with the uniaxial stress-strain data, the Poisson ratio had to be given as input to calculate the shear stresses to which graphite is subject. A review of the literature [44] provided a range of possible values attributable to nuclear-grade graphite between 0.17 and 0.23. Both extremes were

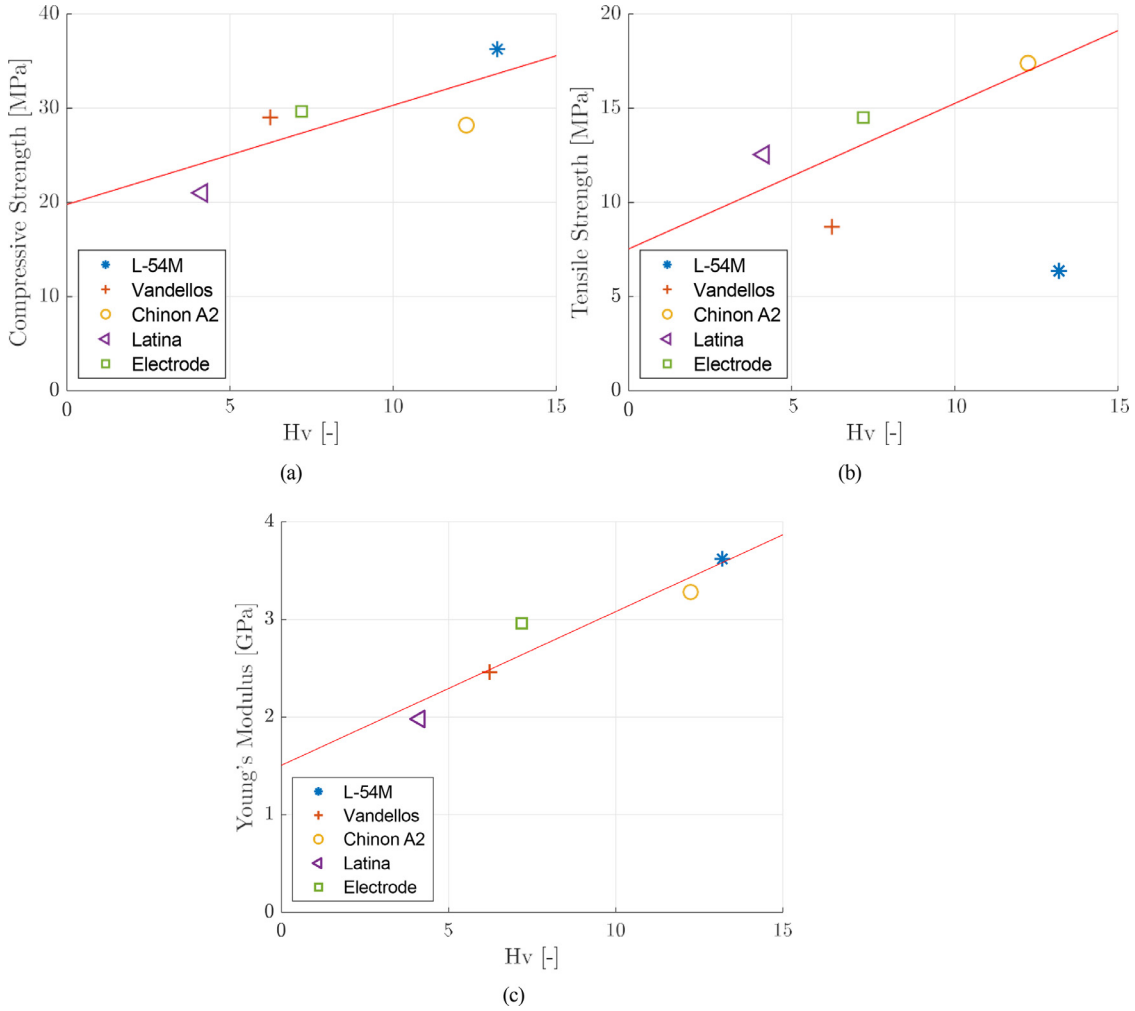

Fig. 5. Graphite mechanical properties correlation of Vickers hardness with (a) compression, (b) tension and (c) Young's modulus.

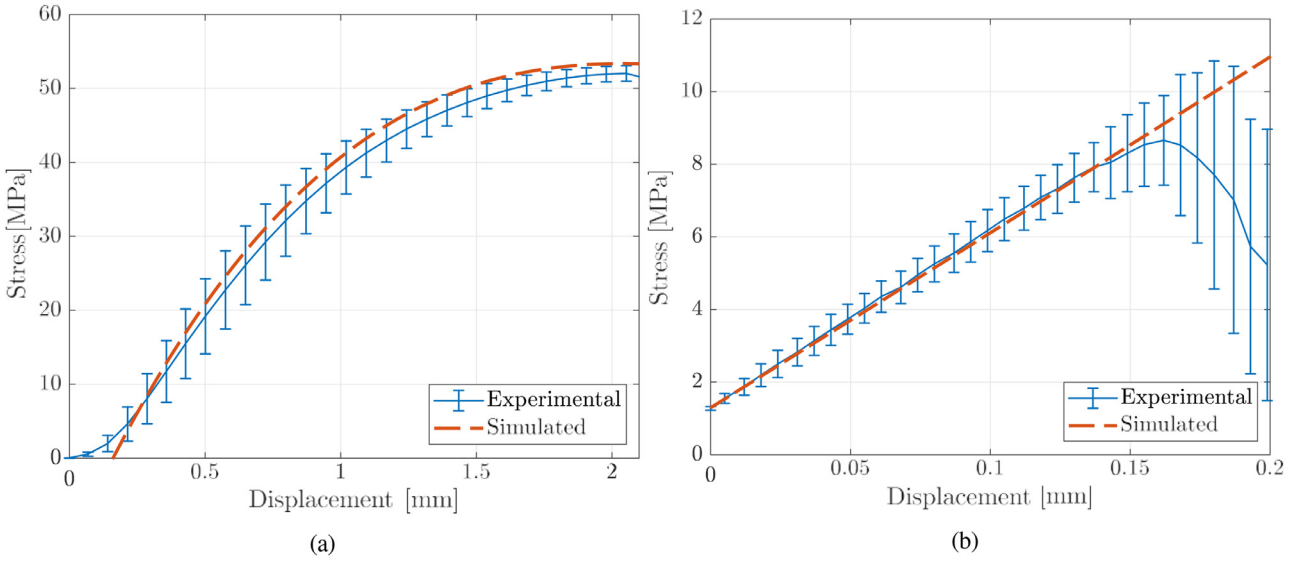

Fig. 6. Non-linear structural model fitting (a) compression and (b) tensile stress-strain curve.

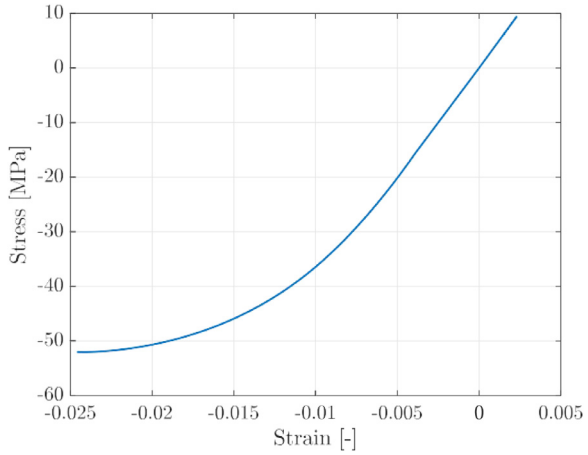

Fig. 7. L-54 M graphite asymmetric stress-strain curve.

tested, and the former gave the most accurate results. Subsequently, the two experimental setups were recreated in COMSOL environment [45]. The geometries were developed to follow the sample geometry for four-point bending and uni-axial compression. The compression test was simulated by constraining the bottom surface and applying a displacement to the top surface equal to the fracture displacement. The same procedure was undertaken for the four-point bending simulation where the constraints were inserted at the location of the lower span and the displacement was applied at the location of the upper span. The results are shown in Figs. 8 and 9. The meshes created for both tests are made up of quadrilateral elements. The choice of said elements over triangular ones was given by the fact that the former can achieve better results in higher-order schemes and maintain better numerical stability and accuracy. Moreover, the simple geometry of the studied samples did not require complex meshes. The developed model cannot predict when fracture can occur; therefore, the stress condition at the mean displacement where the graphite samples broke was evaluated (2 mm for compression and 0.16 mm for four-point bending). The results give a maximum compressive stress of 66.4 MPa and a tensile stress of 9.5 MPa.

Table 4
Comparison between a linear symmetric stress-strain curve graphite model and the modified version.

Graphite	Symmetric Curve [MPa]	Non-Symmetric Curve [MPa]	Experimental [MPA]
Compression			
Magnox	145.2	56.3	21.8
AGOT	105.1	66.4	52.0
Tension			
Magnox	15	14	14.4
AGOT	11.1	9.5	9.5

5.3. Magnox graphite FEM model

The same test procedure was performed on second-generation Pile Grade A (PGA) graphite from Magnox reactors. For tensile strength, the four-point bending approach was performed on 7 samples. The compression data was obtained in a confidential manner by SOGIN (Società Gestione Impianti Nucleari), the Italian enterprise responsible for nuclear decommissioning. The tests were performed on 13 samples with a height-to-diameter ratio close to 1, despite the fact that the ASTM standard requires a ratio of at least 2 for representative bulk behavior [46]. The stress-strain curve values were obtained through image processing using the ImageJ software [47]. The average maximum stress was found to be 21.8 ± 1.2 MPa. The relative standard deviation of this case is observed to be more than double that of AGOT graphite, despite using more samples. The approximate Young's modulus was found to be around 5 GPa, which is consistent with the data available in literature [48]. Table 4 summarizes the results and compares them with a symmetric curve based on the calculated Young's modulus for the two graphite types. The default stress-strain curve within COMSOL is constructed based on the assumption of linearity and symmetry, with the angular coefficient representing Young's modulus. The Magnox graphite model substantially reduces the error, but still overestimates considerably when compared to AGOT. The absence of information on sample orientation and non-standard geometry, as well as the optical image processing of stress-strain curves, significantly diminishes

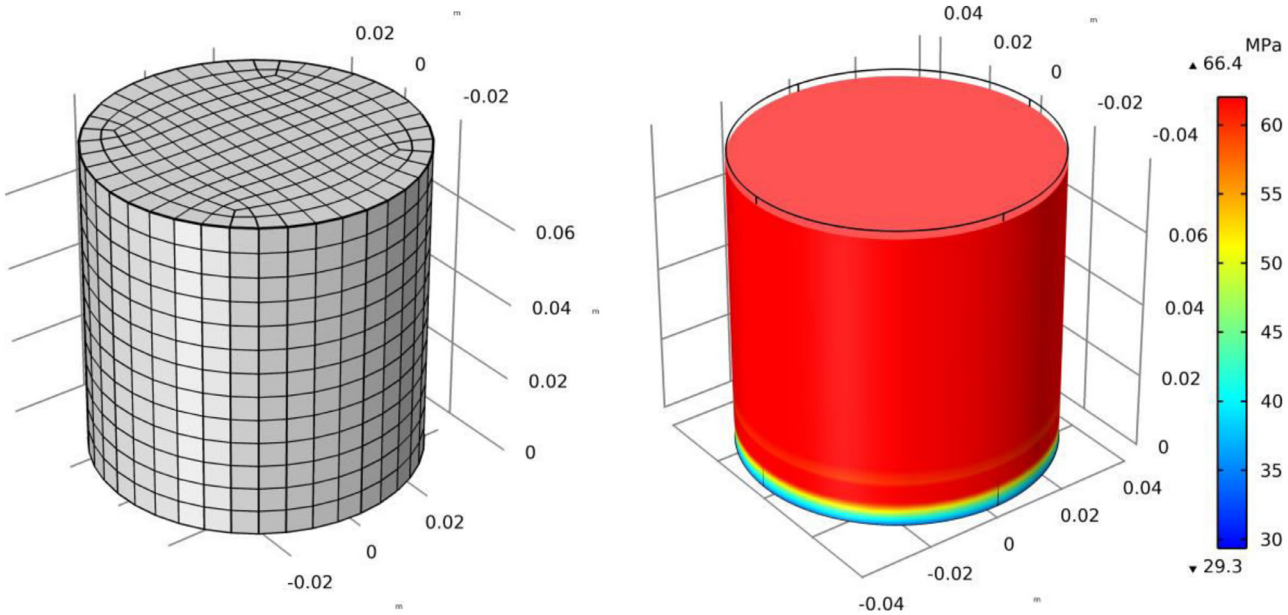

Fig. 8. Compression test recreation in COMSOL.

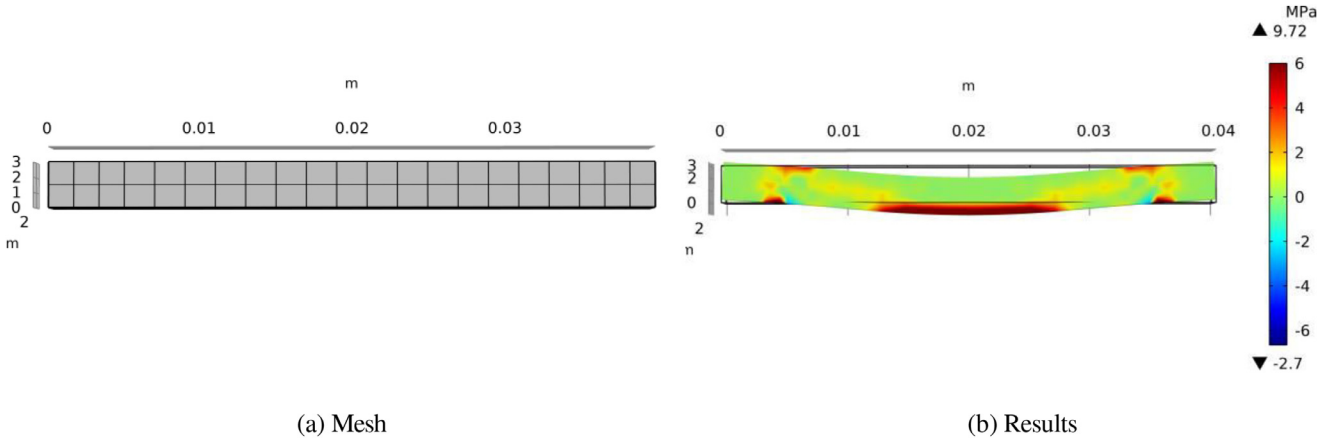

Fig. 9. four-point bending test recreation in COMSOL.

the quality of the results, as evidenced by the higher relative standard deviation.

Conclusions

Significant challenges still need to be addressed in order to ensure a safe, efficient, and cost-effective decommissioning process of graphite-moderated nuclear reactors. Plant characterization is one of the main bottlenecks which requires optimization in order to achieve the project end state within a reasonable time frame and budget. In this work, novel solutions have been proposed to facilitate the mechanical characterization process of nuclear-grade graphite without losing accuracy. ASTM norms served as a starting point and were then modified to better suit the characterization needs. The results of the three-point bending tests were compared to the reference standard of four-point bending, and a correction factor was determined to normalize them. The use of three-point bending enabled both flexion and compression characterization by only using one set of specimen. Two non-linear structural models have been developed to aid in this characterization by estimating with high reliability Young's modulus. Additionally, Vickers microhardness tests confirmed Young's modulus calculation of the non-linear structural model and provided three correlations that could be used to easily and rapidly estimate graphite mechanical properties. Studies are already underway to improve the correlations by taking into account the anisotropy of the properties which have been shown to vary by a factor of roughly 30% depending on graphite extrusion direction. Improved predictive capabilities of FEM graphite models were achieved by introducing the asymmetric stress-strain curve as input data. The FEM model is now intended to be used as a simulator to evaluate stresses arising in graphite bricks under various loads. The implementation of this model will likely be applicable during the assessment of various graphite handling scenarios during decommissioning. This model, together with the Vickers microhardness correlation, will help provide more comprehensive and reliable analysis without the need for lengthy characterization, resulting in a more informed and streamlined decision-making process for graphite-moderated reactors decommissioning.

Declaration of Competing Interest

The authors declare the following financial interests/personal relationships which may be considered as potential competing interests:

Riccardo Chebac reports financial support was provided by inno4graph project.

Data Availability

Data will be made available on request.

Acknowledgments

This project has received funding from the Euratom research and training program 2019–2020 under grant agreement No 945273 (Inno4Graph). Disclaimer: This dissemination of results reflects only the authors' view; the Commission is not responsible for any use that may be made of the information it contains.

References

[1] Harry H. Steinhauser, Nuclear engineering: ¡i¿the design of gas-cooled graphite–moderated reactors¡/i¿. d. r. poulter, ed. oxford university press, new york, 1963. xii + 692 pp. illus. $13.45, Science 142 (3597) (1963) 1288–1288.
[2] M.J. Fisher, The fort St. Vrain decommissioning project, Nucl. Engineer 38 (6) (1997) 185–188.
[3] Chris Halliwell, The windscale advanced gas cooled reactor (wagr) decommissioning project a close out report for wagr decommissioning campaigns 1 to 10-12474, Waste Manage. (Oxford) (2012).
[4] Ian P Graham and J.P. Fowler. Decommissioning of western europes oldest reactor. the graphite low energy experimental file (gleep) at ukaea harwell. 1996.
[5] DEEP SOIL POCKETS EXCAVATION. Brookhaven graphite research reactor decommissioning project. 2005.
[6] Progress in Radioactive Graphite Waste Management, International Atomic Energy Agency, Vienna, 2010 Number 1647 in TECDOC Series.
[7] Anthony Wickham, Hans-Ju¨rgen Steinmetz, Patrick O'Sullivan, Michael I Ojovan, Updating irradiated graphite disposal: project 'grapa'and the international decommissioning network, J. Environ. Radioact. 171 (2017) 34–40.
[8] Jo Jo Lee, Jose´ D Arregui-Mena, Cristian I Contescu, Timothy D Burchell, Yutai Katoh, Sudarshan K Loy- alka, Protection of graphite from salt and gas permeation in molten salt reactors, J. Nucl. Mater. 534 (2020) 152119.
[9] Nicolas Zweibaum, Guoping Cao, Anselmo T Cisneros, Brian Kelleher, Michael R Laufer, Raluca O Scarlat, Jeffrey E Seifried, Mark H Anderson, Charles W Forsberg, Ehud Greenspan, et al., Phenomenology, methods and experimental program for fluoride-salt-cooled, high-temperature reactors (fhrs), Prog. Nucl. Energy 77 (2014) 390–405.
[10] B.J. Marsden, A.N. Jones, G.N. Hall, Muhammad Treifi, P.M. Mummery, Graphite as a core material for gener- ation iv nuclear reactors, in: Structural Materials for Generation IV Nuclear Reactors, Elsevier, 2017, pp. 495–532.
[11] Charalampos Andreades, Anselmo T Cisneros, Jae Keun Choi, Alexandre YK Chong, Massimiliano Fratoni, Sea Hong, Lakshana R Huddar, Kathryn D Huff, James Kendrick, David L Krumwiede, et al., Design summary of the mark-i pebble-bed, fluoride salt–cooled, high-temperature reactor commercial power plant, Nucl Technol 195 (3) (2016) 223–238.
[12] Xiang-wen Zhou, Ya-ping Tang, Zhen-ming Lu, Jie Zhang, Bing Liu, Nuclear graphite for high temperature gas-cooled reactors, New Carbon Mater. 32 (3) (2017) 193–204.
[13] T.J. Neubert, J. Royal, and A.R. Van Dyken. The structure and properties of artificial and natural graphite. 1956.
[14] William Windes, Timothy Burchell, and R. Bratton. Graphite technology development plan. 01 2023.
[15] Johannes Fachinger, Werner von Lensa, Tatjana Podruhzina, Decontamination of nuclear graphite, Nucl. Eng. Des. 238 (11) (2008) 3086–3091.
[16] Yumeng Zhao, Yuhao Jin, Shasha Lv, Jie Gao, Zhou Zhou, Toyohiko Yano, Zhengcao Li, The wigner energy and defects evolution of graphite in neutron-irradiation and annealing, Radiat. Phys. Chem. 201 (2022) 110401.
[17] Decommissioning nuclear facilities (2022). https://world-nuclear.org/information-library/nuclear-fuel-cycle/nuclear-wastes/decommissioning-nuclear-facilities.aspx.
[18] https://www.inno4graph.eu/.

[19] Data Analysis and Collection for Costing of Research Reactor Decommissioning, International Atomic Energy Agency, Vienna, 2017 Number 1832 in TECDOC Series.
[20] M.C.R. Heijna, S. de Groot, J.A. Vreeling, Comparison of irradiation behaviour of htr graphite grades, J. Nucl. Mater. 492 (2017) 148–156.
[21] Huali Wu, Ruchi Gakhar, Allen Chen, Stephen Lam, Craig P Marshall, Raluca O Scarlat, Comparative analysis of microstructure and reactive sites for nuclear graphite ig-110 and graphite matrix a3, J. Nucl. Mater. 528 (2020) 151802.
[22] Hideki Kamide, Gilles Rodriguez, Philippe Guiberteau, Nobuchika Kawasaki, Branislav Hatala, Alessandro Alemberti, Stephane Bourg, Yanping Huang, Frederic Serre, Michael A Fuetterer, et al., Technical report, Organisation for Economic Co-Operation and Develop- ment, 2021.
[23] W.L. Greenstreet, J.E. Smith, G.T. Yahr, Mechanical properties of egcr-type agot graphite, Carbon N Y 7 (1969) 15–45 2.
[24] J.M. Corum, A determination of the fracture toughness of egcr-type agot graphite, J. Nucl. Mater. 22 (1) (1967) 41–54.
[25] E. Mossini, L. Codispoti, M. Giola, L. Castelli, E. Macerata, A. Porta, F. Campi, M. Mariani, Topsoil radio- logical characterisation of l-54m reactor surroundings preliminary to decommissioning operations, J. Environ. Radioact. 196 (2019) 187–193.
[26] B.J. Marsden, Technical Report, 2001.
[27] *Graphite moderator lifecyle behavior*. Number 901 in TECDOC Series, INTERNATIONAL ATOMIC ENERGY AGENCY, Vienna, 1996.
[28] M.L. Ted Guo, C.-.Y.A. Tsao, Tribological behavior of self-lubricating aluminium/sic/graphite hybrid composites synthesized by the semi-solid powder-densification method, Compos. Sci. Technol. 60 (1) (2000) 65–74.
[29] L. Vergari, J. Quincey, G. Meric de Bellefon, T. Merriman, M. Hackett, R.O. Scarlat, Self-lubrication of nuclear graphite in argon at high temperature, Tribol. Int. 177 (2023) 107946.
[30] F. Mujika, On the difference between flexural moduli obtained by three-point and four-point bending tests, Polym. Test. 25 (2) (2006) 214–220.
[31] Young A Suh, Carol Hornibrook, Man-Sung Yim, Decisions on nuclear decommissioning strategies: histor- ical review, Prog. Nucl. Energy 106 (2018) 34–43.
[32] Committee, Test method for compressive strength of carbon and graphite. Technical report, ASTM International (2021).
[33] Committee, Test method for flexural strength of manufactured carbon and graphite articles using, point loading at room temperature. Technical report, ASTM International, 2020.
[34] Julie Chapman, Technical Report, Idaho National Laboratory (INL), 2010.
[35] Committee, Guide for categorization of microstructural and microtextural features observed in optical micrographs of graphite. Technical report, ASTM International (2021).
[36] Zhoutong He, Lina Gao, Wei Qi, Baoliang Zhang, Xue Wang, Jinliang Song, Xiujie He, Can Zhang, Hui Tang, Rohan Holmes, et al., Molten flinak salt infiltration into degassed nuclear graphite under inert gas pressure, Carbon N Y 84 (2015) 511–518.
[37] T.J. Mays. A new classification of pore sizes. *Studies in surface science and catalysis*, 160(Characterization of Porous Solids VII):57–62, 2007.
[38] Joseph R Davis, Tensile Testing, ASM international, 2004.
[39] Eung Seon Kim, Ji Seon Song, Sung Deok Hong, and Yong Wan Kim. Porosity of nuclear grade graphite. Proceedings of the KNS spring meeting, pages 1CD–ROM, Korea, Republic of, 2012. KNS. Specific Nuclear Reactors and Associated Plants (2012).
[40] E. Solfiti, F. Berto, Mechanical properties of flexible graphite, Procedia Struct. Integr. 25 (2020) 420–429.
[41] Harry Chandler, et al., Hardness Testing, ASM international, 1999.
[42] Gian Luca Ghiringhelli, Pierangelo Masarati, Paolo Mantegazza, Multibody implementation of finite volume c beams, AIAA J. 38 (1) (2000) 131–138.
[43] Pierangelo Masarati, Marco Morandini, and Paolo Mantegazza. An efficient formulation for general-purpose multibody/multiphysics analysis. 2014.
[44] https://www.azom.com/properties.aspx?ArticleID=516.
[45] https://www.comsol.com/.
[46] Ergu¨n Tuncay, Nilsun Hasancebi, The effect of length to diameter ratio of test specimens on the uniaxial compressive strength of rock, Bull. Eng. Geol. Environ. 68 (2009) 491–497 11.
[47] https://imagej.net/ij/.
[48] Graphite technology course. Available at https://chrome-extension://https://www.nrc.gov/docs/ML0120/ML012080125.pdf.